Cracking and stress redistribution in ceramic layered composites

K. S. Chan
Southwest Research Institute, San Antonio, TX 78238-5100 (USA)
M. Y. He
Materials Department, University of California, Santa Barbara, Santa Barbara, CA 93106 (USA)
J. W. Hutchinson
Division of Applied Sciences, Harvard University, Cambridge, MA 02138 (USA)

(Received November 16, 1992)

Abstract

Problems are analyzed that have bearing on cracking and survivability in the presence of cracking of layered composite materials composed of brittle layers joined by either a weak interface or a thin layer of a well-bonded ductile metal. The problems concern a crack in one brittle layer impinging on the interface with the neighbouring brittle layer and either branching, if the interface is weak, or inducing plastic yielding, if a ductile bonding agent is present. For the case of a weak interface, the effect of debonding along the interface is analyzed and results for the stress redistribution in the uncracked layer directly ahead of the crack tip are presented. Debonding lowers the high stress concentration just across the interface, but causes a small increase in the tensile stresses further ahead of the tip in the uncracked layer. A similar stress redistribution occurs when the layers are joined by a very thin ductile layer that undergoes yielding above and below the crack tip, allowing the cracked layer to redistribute its load to the neighbouring uncracked layer. The role of debonding and yielding of the interface in three-dimensional tunnel cracking through an individual layer is also discussed and analyzed. Residual stress in the layers is included in the analysis.

1. Introduction

When layered, thin sheets of a brittle material may have toughness and strength properties far superior to those of the material in bulk form [1–6]. To enable good strength and toughness, the interface between adjoining layers must counteract the stress concentration effect of any crack that occurs in an individual layer, reducing the likelihood that it will propagate into the next layer. Depending on the nature of the interface, this may occur by debonding, when the interface is brittle and relatively weak, or by yielding and sliding for systems composed of brittle layers alternating with thin ductile adhesive layers. The latter category is represented by sheets of Al_2O_3 joined by thin layers of aluminum [2] and by the model system with sheets of Al_2O_3 bonded by epoxy [3]. Some of the issues related to the design of layered brittle materials are similar to those encountered in the design of fiber-reinforced brittle matrix composites, such as the selection of interface toughness to prevent matrix cracks from penetrating the fibers. Other issues are unique to the layered geometry, and this paper addresses a few of them. In particular, the role of yielding or debonding of the interface in defeating cracks in individual layers is analyzed by consideration of the stress redistribution in the adjoining uncracked layer that accompanies these processes. Results are given for the energy release rate of three-dimensional cracks tunneling through an individual layer. This release rate, which is influenced by interface yielding or debonding, provides the essential information needed to predict the onset of widespread layer cracking in terms of the thickness of the brittle layer material and its toughness.

The geometries of the problems to be studied are shown in Fig. 1. Figure 1(a) shows a cracked layer of width $2w$ with zones of either yielding or debonding in the interface extending a distance d above and below the crack tips. The interface is taken to be either a very thin ductile layer of an elastic–perfectly plastic material with shear flow stress τ or a weak plane that debonds and slips under conditions such that the layers remain in contact and exert a friction stress τ on each other. The ductile adhesive layer allows relative slipping of the layers it joins by plastic yielding, but it is assumed that debonding does not occur. In this case, the condition $K_2 = 0$ must be enforced, leading to well-behaved shear stresses at the end of the yielding zone and estab-

0921-5093/93/$6.00
© 1993 – Elsevier Sequoia. All rights reserved

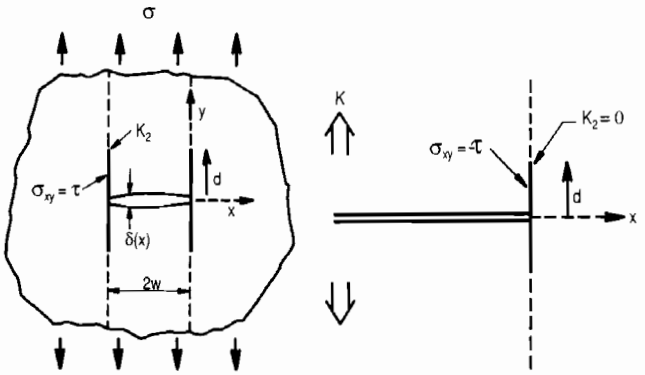

Fig. 1. Specification of the plane strain problems: (a) finite layer crack; (b) asymptotic problem.

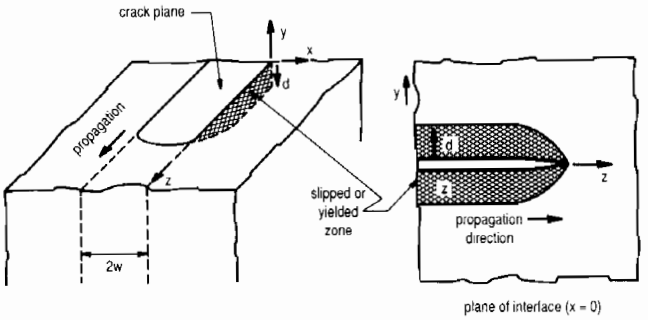

Fig. 2. Specification of the three-dimensional tunneling crack problem.

lishing the zone length d. In the case where the interface debonds, the interface crack is fully closed for $d/w > 0.71$ [7]. The mode 2 stress intensity factor K_2 at the end of the slipped zone will be nonzero, and must attain the mode 2 toughness of the interface for the debond to spread. Results for K_2 are given below.

Cracks in individual layers spread as three-dimensional tunnel cracks propagating through the layer (Fig. 2). Once the crack has spread a distance of at least several layer thicknesses in the z direction it approaches a steady state wherein the behavior at the propagating crack front becomes independent of the length of the crack in the z direction. Under these steady-state conditions, the energy release rate of the propagating front can be computed by use of the plane strain solution associated with the geometry of Fig. 1(a) (other examples of tunnel cracks are given in ref. 8). The steady-state energy release rate can be computed in terms of the average of the opening $\delta(x)$ of the plane strain crack. The zone of yielding or debonding increases the tunneling energy release rate, thereby lowering the overall stress at which widespread layer cracking can occur. Results for the tunneling energy release rate are given below. The role of residual stresses in the layers are readily accounted for: this is discussed in the final section.

When the interface is weak and debonding occurs, the interface crack is fully open with mixed mode intensity factors when $d/w < 0.24$ [7]. This case can be approximated well by the asymptotic problem for a semi-infinite crack impinging the interface where the remote field is the K-field associated with the problem in Fig. 1(a), with $d = 0$. The stress redistribution in the next layer ahead of the impinging crack tip is given, with a correction of previous energy release rate results for the doubly-deflected interface crack [9]. When plastic yielding of a ductile adhesive layer occurs, another asymptotic problem applies when σ is sufficiently small compared with τ. Then, the asymptotic problem is that shown in Fig. 1(b) for a semi-infinite crack loaded remotely by the same K-field. In this case also, the effect of yielding in the thin adhesive layer on the stress distribution ahead of the crack tip in the uncracked layer is emphasized.

2. Effect of plastic yielding on stress redistribution

As discussed above, the thin ductile adhesive layers in Fig. 1(a) are assumed to be elastic–perfectly plastic with a yield stress in shear of τ, and are modeled as having zero thickness. The plane strain problem is considered where the central cracked layer has the same elastic properties (E, ν) as the semi-infinite blocks adjoining across the interfaces. Under monotonic increase of the applied remote stress σ, the zones of yielding of half-height d spread allowing slip in the form of a tangential displacement discontinuity across the interface in the yielded region. The condition $\sigma_{xy} = \pm\tau$ is enforced within the yielded zones of the interface. The Dugdale-like condition $K_2 = 0$ at the ends of the yielded zones ensures that the shear stress on the interface falls off continuously just outside the yielded zone, and it determines the relation of d/w to σ/τ under the monotonic loading considered. Integral equation methods are employed to solve this problem as well as the others posed below; the methods used are outlined briefly in Appendix A.

The two most important functional relations needed to solve the three-dimensional tunneling crack problem discussed below are shown in Figs. 3 and 4. In Fig. 4, $\bar{\delta}$ is the average crack opening displacement defined by

$$\bar{\delta} = \frac{1}{2w} \int_{-w}^{w} \delta(\xi)\, \delta\xi \tag{1}$$

The elastic value of $\bar{\delta}$, valid when there is no yielding $(\tau \to \infty)$, is $\bar{\delta}_0 = \pi(1-\nu^2)\sigma w/E$. Yielding of the adhesive layers begins to make a significant contribution to the

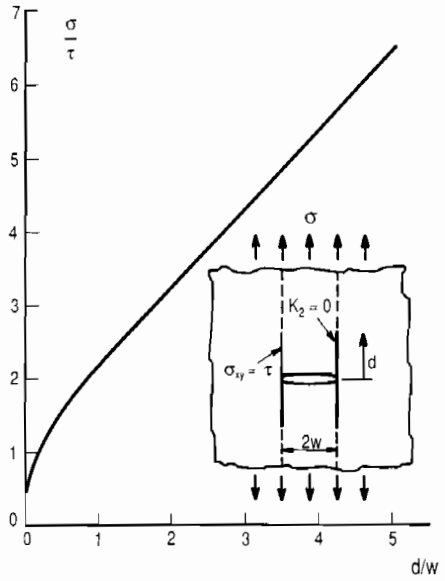

Fig. 3. Relation between applied stress and height of the yielding zone in a thin ductile adhesive layer.

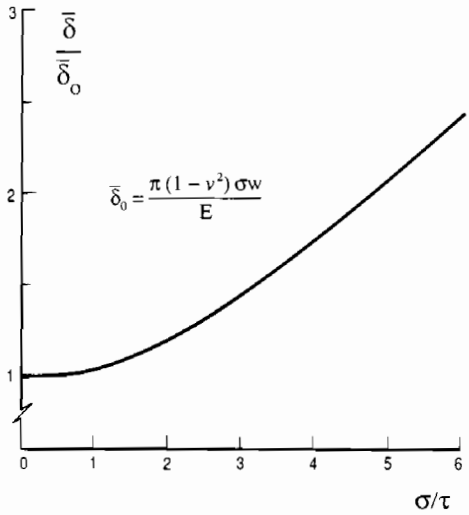

Fig. 4. Average crack opening displacement as a function of the ratio of applied stress to shear yield stress of the thin ductile adhesive layer.

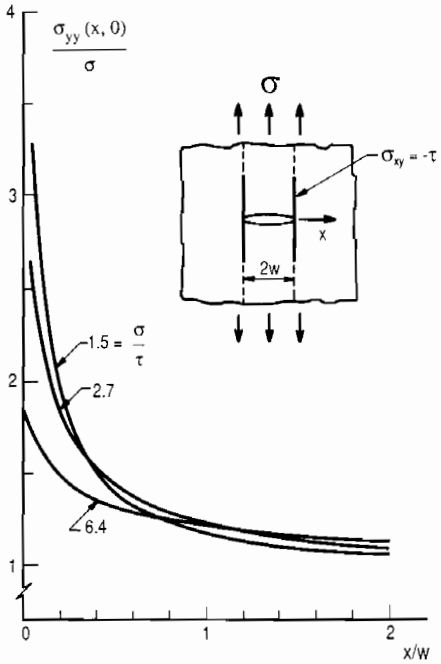

Fig. 5. Stress distribution ahead of the crack tip in the uncracked layer at several levels of applied stress to shear yield stress of the thin adhesive layer.

average crack opening displacement when σ/τ exceeds unity. The redistribution of normal stress $\sigma_{yy}(x, 0)$ in the block of material across the interface is shown in Fig. 5 for three levels of σ/τ. The curve shown for $\sigma/\tau = 1.5$ is only very slightly below the elastic distribution

$$(\sigma_{yy}(x, 0) = (\bar{x} + 1)/(\bar{x}^2 + 2\bar{x})^{1/2}$$

for $\bar{x} \equiv x/w > 0.05$. Reduction of stress ahead of the crack tip begins to be appreciable when $\sigma/\tau = 2.7$, and is quite significant when $\sigma/\tau = 6.4$. The drop in stress just across the interface is offset by a slight increase in stress relative to the elastic distribution further from the interface. This feature is seen in all the stress redistribution results.

Stress redistribution can be presented in another way when d/w is sufficiently small, by use of the asymptotic problem shown in Fig. 1(b). Provided d/w is sufficiently small, the yielding behavior is small-scale yielding with the elastic stress intensity factor K as the controlling load parameter. The remote field imposed on the semi-infinite crack is the elastic K-field. This asymptotic problem has also been solved with integral equation techniques. The extent of the yield zone in the asymptotic problem is

$$d = 0.052 \left(\frac{K}{\tau}\right)^2 \tag{2}$$

Figure 6 displays the normal stress directly ahead of the crack tip in the adjoining block normalized by the elastic stress field for the limit $\tau = \infty$. The stress ratio in Fig. 6 depends on x/d but is otherwise independent of K in the asymptotic problem. Yielding reduces the stress below the elastic level over a region ahead of the crack tip which is slightly larger than $d/10$. Beyond that region the stresses are slightly elevated above the elastic levels and approach the elastic distribution as x/d becomes large. The stress redistribution due to debonding (Fig. 6) is more dramatic: this is discussed below.

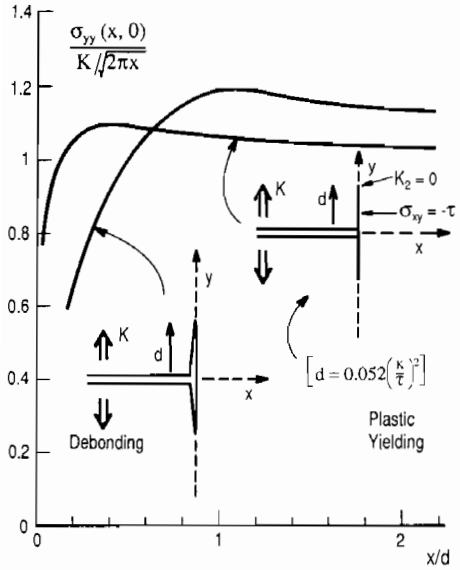

Fig. 6. Stress redistribution ahead of the crack tip in the layer across the interface for the two asymptotic problems ($d \ll w$).

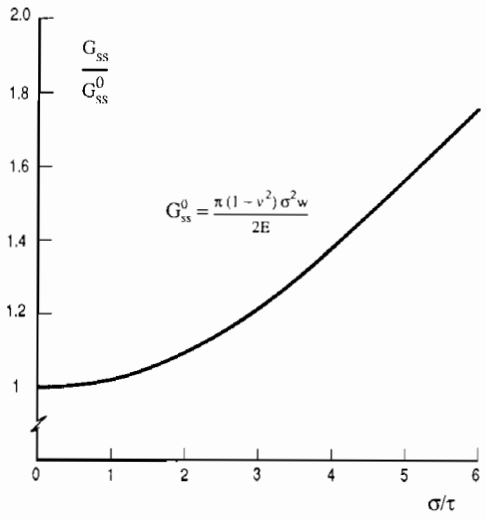

Fig. 7. Normalized steady-state energy release rate for the tunneling crack in the case of thin ductile adhesive layers with shear yield stress τ.

3. Effect of plastic yielding on tunnel cracking

As stated above, the steady-state energy release rate for a three-dimensional tunneling crack can be computed by use of the plane strain solution. For the geometry and loading shown in Figs. 1(a) and 2, the leading edge of the tunneling crack propagating in the z direction experiences mode 1 conditions. Let G_{ss} denote the energy release rate averaged over the propagating crack front. An energy balance accounting for the release of energy per unit advance of the tunnel crack under steady-state conditions gives $2wG_{ss}$ as the work done by the tractions acting across the plane of the layer crack in the plane strain problem as those tractions are reduced to zero from σ. For the present problems, this is the same as

$$G_{ss} = \int_0^{\sigma} \bar{\delta}(\sigma')\, d\sigma' \tag{3}$$

where $\bar{\delta}$ is the average crack opening displacement for the traction-free plane strain crack under monotonically increased remote σ. The elastic result for $d=0$ (*i.e.* $\tau=\infty$) is

$$G_{ss}^0 = \frac{\pi(1-\nu^2)\sigma^2 w}{2E} \tag{4}$$

The ratio of G_{ss} to G_{ss}^0 can be computed from the data in Fig. 4 by use of simple numerical integration. The result is plotted in Fig. 7. Increases of the steady-state release rate above the elastic value become important when σ/τ exceeds unity.

4. Effect of debonding and frictionless slipping on stress redistribution

The plane strain interface debonding problem for the geometry of Fig. 1(a) is as follows for the case where no frictional resistance is exerted across the debonded interfaces (*i.e.* $\tau=0$). According to ref. 7, the debonded interface will be fully open when $d/w<0.24$, and the interface crack tip at the end of the debond is subject to mixed mode conditions, as discussed for the asymptotic problem below. For $0.24<d/w<0.71$, the debond crack tip is closed and therefore in a state of pure mode 2, but a portion of the interface near the main layer crack is still open. For $d/w>0.71$, the interface is fully closed and the interface crack tip is in mode 2. The top curve for the normalized mode 2 stress intensity factor in Fig. 8 applies to the frictionless case. It was computed using the integral equation methods outlined in Appendix A under the constraint that the interface remains closed. The results are strictly correct only for $d/w>0.71$ (and agree with the results of ref. 7), but are only slightly in error for smaller d/w. The average crack opening displacement $\bar{\delta}$ needed for the tunnel crack calculations is shown in Fig. 9, where the top curve again applies to the frictionless case.

The role of debonding on stress redistribution is seen in Fig. 10, where curves of the stress ahead of the right-hand layer crack tip (normalized by the remote applied stress σ) are plotted for various levels of debonding, all for the closed interface with $\tau=0$. Debonding clearly has a significant effect on lowering of the stress on the adjoining material just across the interface; more so than for plastic yielding of a thin

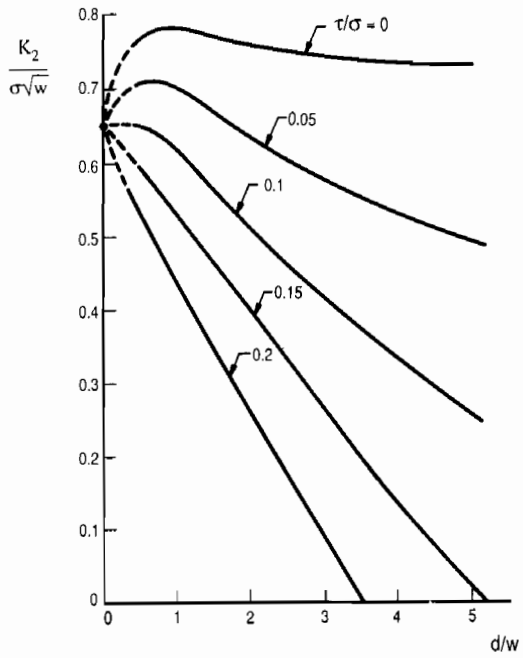

Fig. 8. Normalized mode 2 stress intensity factor for the debonding interface crack at several levels of interface friction stress to applied stress.

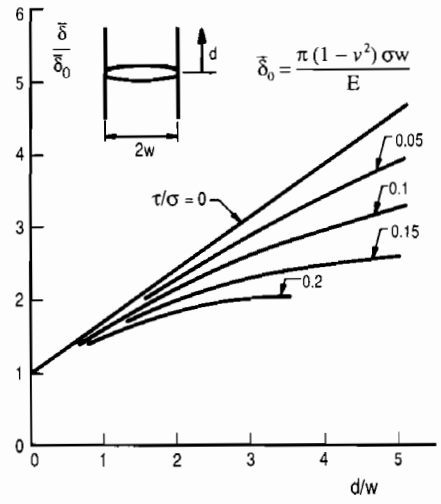

Fig. 9. Average crack opening displacement as a function of debond length at several levels of interface friction stress to applied stress.

ductile layer discussed in connection with Fig. 5. For sufficiently small d/w, the debonded interface is fully open and the asymptotic problem for a semi-infinite crack impinging on the interface applies, as shown in the insert in Fig. 6. The stress redistribution is plotted in Fig. 6, which shows that the stress ahead of the layer crack tip is reduced below the level in the absence of debonding over a distance from the interface equal to half the debond length d. Figure 6 also shows that debonding appears to be more effective in protecting

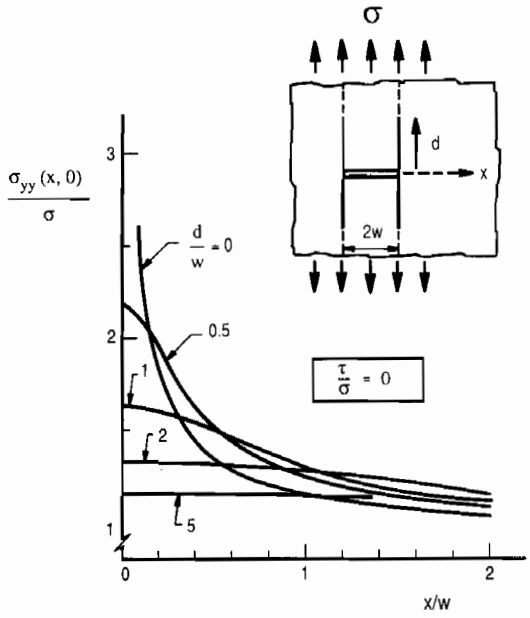

Fig. 10. Stress distribution ahead of the crack tip in the uncracked layer across the interface for the case of no interface friction.

the uncracked layer across the interface than plastic yielding of a thin ductile adhesive layer.

As a digression, the mode 1 and 2 stress intensity factors are recorded for the open interface crack tip for the asymptotic problem of Fig. 6

$$\frac{K_1}{K} = 0.399$$

and (5)

$$\frac{K_2}{K} = 0.322$$

The associated ratio of the energy release rate of the interface crack tip to that of a mode 1 crack penetrating straight through the interface without debonding is 0.263 when both the deflected tips and the penetrating tip emerge from the main crack tip at the same applied K. These results correct results given in ref. 9 that were in error for the case of the doubly-deflected interface crack. A complete set of corrections of this energy release rate ratio for this case over the full range of elastic mismatch across the interface is given in ref. 10.

5. The effect of frictional slipping on debonding and tunnel cracking

Figures 8 and 9 show curves for the normalized mode 2 stress intensity factor and the average crack

opening displacement respectively in the plane strain problem for several levels of a constant friction stress τ relative to σ acting over the bonded interface. A constant friction stress, as opposed for example to a Coulomb friction stress, has been used by some workers to represent the frictional forces exerted across slipping interfaces in composites. The purpose of the present limited study is to illustrate the effect of friction in establishing the extent of debonding and its associated influence on the three-dimensional tunneling energy release rate. Almost certainly, additional studies will be required before understanding is good, including studies with other friction laws. Some results for the effect of Coulomb friction on the mode 2 interface stress intensity factor are given in ref. 11.

Let K_c denote the mode 2 toughness of the interface. Attention will be concentrated on the behavior following initiation of interface debonding when the debond length d is sufficiently large (*i.e.* greater than $\sim w/4$) such that the debond interface crack tip is in mode 2. Impose the debonding condition $K_2 = K_c$ on the solution presented in Figs. 8 and 9. The relationships of the applied stress with the debonding length and the average crack opening displacement that result are plotted in Figs. 11 and 12. The two nondimensional stress parameters in these figures are the applied stress parameter $\sigma(w)^{1/2}/K_c$ and the constant friction stress parameter $\tau(w)^{1/2}/K_c$. (It is necessary to interpolate values between the curves of Figs. 8 and 9 to arrive at the plots in Figs. 11 and 12, since a constant value of $\tau(w)^{1/2}/K_c$ does not correspond to a constant value of τ/σ.) In the range of d less than $\sim w/4$, the predictions are not expected to be correct since the interface undergoes mixed mode debonding and not mode 2 debonding. Thus, the details in the vicinity of the initiation of debonding are not correct. In particular, the value of $\sigma(w)^{1/2}/K_c$ at which $\bar{\delta}$ begins to depart from $\bar{\delta}_0$ (see Fig. 12) would depend on the mixed mode condition for debond initiation. But once debonding has progressed to the point that the interface crack tip is closed, the mode 2 criterion is appropriate and the curves are accurate.

In the absence of friction the debonding process is unstable, since for a fixed σ, K_2 has a maximum when $d \approx w$ and then drops slightly to an asymptote as d increases further. Under a prescribed σ, the mode 2 debond would advance dynamically after it was initiated. In this sense, the curves shown in Figs. 11 and 12 for $\tau = 0$ represent unstable debonding behavior. Friction stabilizes the debonding process, giving rise to a monotonically increasing debond length and average crack opening displacement as the applied stress increases A nondimensional friction stress of the order of $\tau(w)^{1/2}/K_c = 1/8$ or more is required if friction is to be important.

The steady-state energy release rate for tunnel cracking can be computed from the curves in Fig. 12 using eqn. (3). The results of this calculation are plotted in Fig. 13. As before, G_{ss} is normalized by the value for a layer crack with no debonding given in eqn. (4). The above remarks on accuracy in the vicinity of debond initiation also apply to these curves. It can be seen from Fig. 13 that debonding can significantly promote tun-

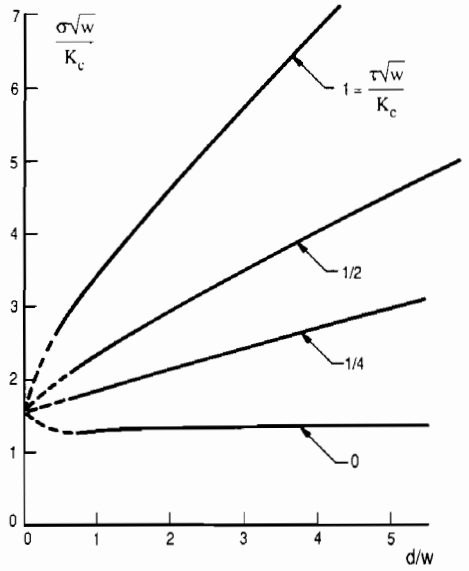

Fig. 11. Relation of normalized applied stress and debond height at several levels of the non-dimensional interface friction stress: the condition $K_2 = K_c$ is imposed, where K_c is the mode 2 interface toughness.

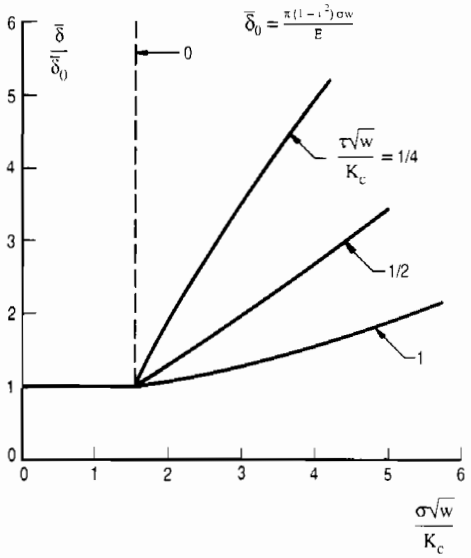

Fig. 12. Relation of the average crack opening displacement and normalized applied stress at several levels of the nondimensional interface friction stress: the condition $K_2 = K_c$ is imposed, where K_c is the mode 2 interface toughness.

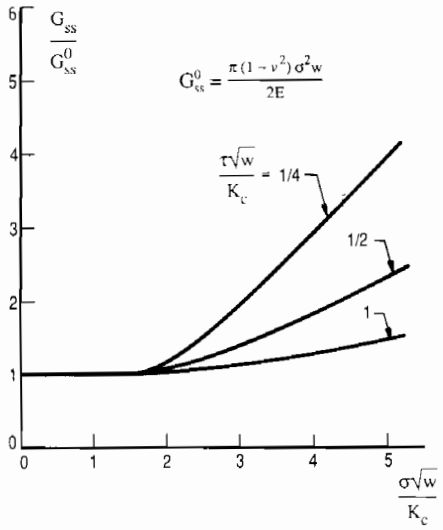

Fig. 13. Steady-state energy release rate for the tunneling crack: the condition $K_2 = K_c$ is imposed, where K is the mode 2 interface toughness.

neling cracking when the nondimensional friction stress is less than about $\tau(w)^{1/2}/K_c = 1/2$.

6. Accounting for residual stress in the cracked layer

The role of a uniform residual tension $\sigma_{yy} = \sigma_R$ preexisting in the layer that undergoes tunnel cracking can readily be taken into account in the various results presented above. For the purpose of discussion, let $\sigma_{yy} = \sigma_A$ be the applied stress, replacing the notation for σ given above. The results in Figs. 3, 4, 7–9 and 11–13 apply as they stand if σ is identified with $\sigma_A + \sigma_R$. The results for stress redistribution shown in Figs. 5 and 10 can also be used, with the following modifications. With σ identified with $\sigma_A + \sigma_R$, the results in Figs. 5 and 10 are correct for the *change* in σ_{yy} in the layer ahead of the tip due to cracking if the numerical value of the ordinate is reduced by 1. To obtain the total stress σ_{yy} in the layer in question, one must then add the *change* and the stress σ_{yy} existing in the layer prior to the cracking event.

Acknowledgments

The work of K. S. Chan was supported by the Internal Research Program, Southwest Research Institute, San Antonio, Texas. The work of M. Y. He was supported by the DARPA URI at the University of California, Santa Barbara (ONR Contract N00014-86-K-0753). The work of J. W. Hutchinson was supported in part by the DARPA URI (Subagreement P.O. # VB38639-0 with the University of California, Santa Barbara, ONR Prime Contract N00014-86-K-0753) and by the Division of Applied Sciences, Harvard University.

References

1 D. B. Marshall and J. J. Ratto, *J. Am. Ceram. Soc., 74* (1991) 2979–2987.
2 H. C. Cao and A. G. Evans, *Acta Metall. Mater., 39* (1991) 2997.
3 C. A. Folsom, F. W. Zok, F. F. Lange and D. B. Marshall, *J. Am. Ceram. Soc., 75* (1992) 2969–2975.
4 B. J. Dalgleish, K. P. Trumble and A. G. Evans, *Acta Metall. Mater., 37* (1989) 1923–1931.
5 M. C. Shaw, D. B. Marshall, M. S. Dadkhah and A. G. Evans, Cracking and damage mechanisms in ceramic/metal multilayers, *Acta Metall. Mater.*, in press.
6 M. Y. He, F. E. Heredia, D. J. Wissuchek, M. C. Shaw and A. G. Evans, *Acta Metall. Mater., 41* (1993) 1223–1228.
7 A. Dollar and P. S. Steif, *J. Appl. Mech., 58* (1991) 584–586.
8 J. W. Hutchinson and Z. Suo, Mixed mode cracking in layered materials, *Adv. Appl. Mech., 29* (1991) 63–191.
9 M. Y. He and J. W. Hutchinson, *Int. J. Solids Struct., 25* (1989) 1053–1067.
10 M. Y. He and J. W. Hutchinson, The effect of residual stress on the competition between crack deflection and penetration at an interface, to be published.
11 A. Dollar and P. S. Steif, *J. Appl. Mech., 56* (1989) 291–298.

Appendix A: Numerical approaches

Two integral equation formulations were used in the solution of the problems discussed. As these have been used by various authors to solve related plane strain problems, details of the methods are not given here. In some cases, results were generated by use of both schemes as a check. The methods used for the problems for the closed interface cracks at the ends of the finite length layer crack (see Fig. 1(a)) are discussed first.

The integral equations in method 1 are formed by representation of both the layer crack and the mode 2 interface cracks in terms of distributions of dislocations. With reference to Fig. 1(a), let $b_o(x) = -d\delta_y/dx$ denote the amplitude of the dislocation opening distribution extending from 0 to w along $y = 0$, and let $b_s(y) = -d\delta_y/dy$ denote the amplitude of the dislocation shearing distribution along $x = w$ extending from 0 to d. The condition that $\sigma_{yy} = 0$ along $y = 0$ for $-w < x < w$ can be written as

$$\int_0^w H_1(x, x')b_0(x')\,dx' + \int_0^d H_2(x, y)b_s(y)\,dy = -\sigma \qquad (6)$$

where $H_1(x, x')$ denotes the stress $\sigma_{yy}(x)$ along $y = 0$ due to $b_0(x')$, with due regard for the symmetry of this distribution with respect to $x = 0$, and $H_2(x, y)$ denotes $\sigma_{yy}(x)$ due to $b_s(y)$, with the appropriate four-fold

symmetry on this distribution imposed. Similarly, the condition that $\sigma_{xy} = -\tau$ along $x = w$ between 0 and d (with the corresponding shear conditions met along the other three legs of the H-crack) is

$$\int_0^w H_3(y, x')b_0(x')\,dx' + \int_0^d H_4(y, y')b_s(y')\,dy' = -\tau \qquad (7)$$

where $H_3(y, x')$ is $\sigma_{xy}(y)$ along $x = w$ due to $b_0(x')$ and $H_4(y, y')$ is $\sigma_{xy}(y)$ due to $b_s(y')$.

Method 2 uses the solution for the problem of four symmetrically placed dislocations interacting with a traction-free crack extending along the x-axis from $-w$ to w. With $H(y, y')$ denoting the shear stress $\sigma_{xy}(y)$ along $x = w$ between 0 and d due to $b_s(y')$, with due regard for the other three symmetrically placed dislocations, the single integral equation for b_s is

$$\int_0^d H(y, y')b_s(y')\,dy' = -\sigma_{xy}^0(y) - \tau \qquad (8)$$

where $\sigma_{xy}^0(y)$ is the shear stress along $x = w$ due to the remote stress acting on the layer crack in the absence of the interface cracks.

The kernels of the above integrals have Cauchy singularities. The dislocation distributions can be obtained by use of several well known numerical techniques. Once the distributions are known in either method, they can be used with other integral expressions to compute the stress components at any point in the plane and the mode 2 stress intensity factor at the end of the interface crack. For the cases in which K_2 is nonzero, the distribution $b_s(y)$ has an inverse square root singularity at $y = d$, while it diminishes with the square root of the distance from $y = d$ for the plastic yielding problems with $K_2 = 0$. The solutions do not rely on a precise incorporation of the correct behavior of the dislocation distributions at the corner point at $x = w$ on $y = 0$. A number of choices were made, including representations that built in the correct lowest order functional behavior near this point.

The asymptotic problem for the semi-infinite layer crack and the mode 2 interface cracks (see Fig. 1(b)) was solved using method 2. Now, $H(y, y')$ is the shear stress along $x = 0$ between 0 and d due to just two symmetrically placed dislocations on $x = 0$ at $\pm y'$ interacting with a traction-free semi-infinite crack, and $\sigma_{xy}^0(y)$ is the shear stress on $x = 0$ due to the K-field in the absence of the interface cracks. The second asymptotic problem discussed in connection with Fig. 6, in which the interface crack opens, is also solved using method 2, but here both shear dislocations and opening dislocations must be used and the problem becomes a set of dual integral equations. In all the cases involving method 2, the kernel functions H can be obtained in closed form by use of complex variable methods of elasticity.